A Consumer Tracking Estimator for Vehicles in GPS-free Environments

Eunseok Choi and Sekchin Chang

***Abstract*—The global positioning system (GPS) is a crucial component in navigation systems. Therefore, navigation systems usually malfunction in the outage cases of GPS signals. This paper proposes a consumer tracking estimator for vehicles in GPS-free environments. The proposed estimator exploits low-cost inertial measurement unit (IMU) and on-board diagnostics II (OBD-II) of the vehicle in order to achieve navigation data without any aid of GPS. The presented estimator is based on extended Kalman filter and linear Kalman filter for vehicle attitude and 3-D velocity estimations, respectively. For accurate estimations in GPS-free situations, the extended and linear Kalman filters achieve the inertial data and the vehicle speed from the IMU and the OBD-II, respectively. The proposed estimator tracks the vehicle trajectory velocity in GPS-free environments. Experiment results verify that the presented tracking estimator accurately tracks the vehicle trajectory without GPS. The results also exhibit that the proposed tracking estimator is superior to the conventional GPS-based estimators in the tracking performance.**

***Index Terms*—GPS-free, Kalman Filter, Tracking Estimator**

I. Introduction

A lot of attention has been paid to navigation systems for mobile objects such as vehicles. In such navigation systems, the GPS plays a key role for location estimation. However, GPS services are often in an outage state due to severe signal fading in surrounding hills, buildings or tunnel environments. Sometimes, natural or man-made disasters cause the failure of GPS services [1]. To overcome the weak points of GPS, several location estimation schemes have been proposed [2], [3]. However, those approaches are not suitable for tracking of high-speed mobile objects including vehicles. Some navigation systems rely on inertial data as well as GPS measurements in order to overcome the GPS service outage [4]-[6]. For the attitude determination, the inertial-data based methods have widely been studied in various areas such as consumer electronics, defense industry, and augmented reality application [7]-[9]. These studies can mainly be classified into 3 sensor fusion techniques: Euler angle representation, direct cosine matrix (DCM) and quaternion approaches. The sensor fusion methods utilize a low-cost IMU, which produces inertial data. Among the fusion techniques, the Euler angle method exhibits the drawbacks of singularities and intensive computation. In addition, the DCM technique is not suitable for expansion. Therefore, quaternion approach is more preferable in the inertial-data based methods. Using the quaternion technique, the conventional navigation systems enable a trajectory tracking even in the outage cases of GPS service. However, the performance of the navigation systems is affected by the fidelity of GPS information. If the latest GPS information is unreliable when the GPS signal is lost, the navigation systems usually exhibit poor tracking performance.

This paper proposes a novel tracking estimator for vehicles in GPS-free environments. Therefore, the paper does not focus on GPS measurements but inertial data for trajectory tracking of vehicles. The presented estimator exploits the measurement information from OBD-II instead of GPS. Most vehicles are equipped with OBD-II for their self-diagnostic and reporting capability. The OBD-II standard specifies the type of diagnostic connector and its pin-out, the electrical signaling protocols, and the messaging format [10]. For the message communication, the OBD-II client systems (as OBD-II readers) send the diagnostic trouble codes (DTCs) or the parameter identifiers (PIDs), and in return receive real-time information from the electronic control unit (ECU) of vehicle. The DTCs are used to diagnose malfunctions, and the PIDs are used to measure real time parameters. The OBD-II systems have a data link connector (DLC), which is usually at the bottom of dash board and can be connected to OBD-II readers. Using the OBD-II readers, it is possible to obtain vehicle information, which includes intake manifold absolute pressure (MAP), revolutions per minute (RPM), intake air temperature (IAT), mass air flow (MAF) sensor rate, and vehicle speed (VSS). Recently, various OBD-II consumer electronics have been designed and developed, which exploit such vehicle information [11], [12]. The consumer devices rely on the OBD-II in order to perform fleet management [11] and assess driving behaviors [12], respectively. The devices need to accurately estimate vehicles' attitude for effective management and assessment. The proposed approach guarantees the accurate estimation of vehicles' attitude even in the case that GPS signal is unavailable. This is the main benefit of the

Manuscript received September 25, 2017; accepted November 15, 2017. Date of publication December 19, 2017. This research was supported by Research Program through the National Research Foundation of Korea (NRF) (2017R1A2B4005105). *(Corresponding author: S. Chang.)*

Eunseok Choi is with the Department of Electrical and Computer Engineering, the University of Seoul, Seoul, Korea (e-mail: eschoi511@hotmail.com).

Sekchin Chang is with the Department of Electrical and Computer Engineering, the University of Seoul, Seoul, Korea (e-mail: schang213@uos.ac.kr).

Color versions of one or more of the figures in this paper are available online at http://ieeexplore.ieee.org.

Digital Object Identifier 10.1109/TCE.2017.015064

presented method for the consumer devices. The presented estimator obtains inertial data from a low-cost IMU. Then, the estimator employs an extended Kalman filter (EKF) in order to transform the inertial data into the vehicle attitude (pitch, roll, and yaw). The transformation is based on the quaternion approach [7], which is utilized for the presented tracking estimator. In addition to the inertial information, the proposed estimator can achieve the vehicle speed information from the OBD-II as stated earlier. Then, the proposed estimator utilizes a linear Kalman filter (LKF) in order to convert the vehicle speed information of the OBD-II into the 3-D velocity information in the navigation frame of north-east-down (NED). The novel estimator finally estimates the vehicle position using the vehicle attitude and the 3-D velocity information. Therefore, the suggested estimator can track the vehicle trajectory without any aid of GPS service.

Experiment results show that the proposed tracking estimator gives better tracking performance than the conventional GPS-based estimators. They also confirm that the presented estimator can accurately track the vehicle trajectory without any assistance of GPS service.

II. Related Works For Attitude Estimation

For the attitude estimation, two schemes are mainly utilized. One approach estimates the attitude using GPS information as well as quaternion measurements. The other method utilizes only quaternion measurements for the attitude estimation.

A. Attitude Estimation Based On Quaternion and GPS

As one of the related works, section II-A describes the attitude estimation scheme [5], which is based on quaternion and GPS. The attitude quaternion is expressed as:

$$\vec{q} = q_0 + iq_1 + jq_2 + kq_3 = \begin{bmatrix} q_0 & q_1 & q_2 & q_3 \end{bmatrix}^T, \quad (1)$$

where q_0 is the scalar part, and q_1, q_2 and q_3 are the vector parts. This method uses a rotation matrix that can transform navigation frame n into body frame b. In the rotation matrix, the relationship between quaternion vector $\vec{q}$ and zyx sequence can be expressed as:

$$C_n^b = \begin{bmatrix} C_{11} & C_{12} & C_{13} \\ C_{21} & C_{22} & C_{23} \\ C_{31} & C_{32} & C_{33} \end{bmatrix} = \begin{bmatrix} q_0^2+q_1^2-q_2^2-q_3^2 & 2(q_0q_3+q_1q_2) & 2(q_1q_3-q_0q_2) \\ 2(q_1q_2-q_0q_3) & q_0^2-q_1^2+q_2^2-q_3^2 & 2(q_0q_1+q_2q_3) \\ 2(q_0q_2+q_1q_3) & 2(q_2q_3-q_0q_1) & q_0^2-q_1^2-q_2^2+q_3^2 \end{bmatrix}, \quad (2)$$

where C_{11}, C_{22}, and C_{33} can also be expressed as follows:

$$\begin{aligned} C_{11} &= 1-2(q_2^2+q_3^2) \quad or \quad 2(q_0^2+q_1^2)-1 \\ C_{22} &= 1-2(q_1^2+q_3^2) \quad or \quad 2(q_0^2+q_2^2)-1 \\ C_{33} &= 1-2(q_1^2+q_2^2) \quad or \quad 2(q_0^2+q_3^2)-1 \end{aligned}. \quad (3)$$

The transformation between frame n and frame b can be expressed as follows:

$$\begin{aligned} &U_{body} = C_n^b U_{nav},\ U_{nav} = C_b^n U_{body},\ C_b^n = (C_n^b)^T \\ &U_{body} = \begin{bmatrix} U_{bx} & U_{by} & U_{bz} \end{bmatrix}^T,\ U_{nav} = \begin{bmatrix} U_{nx} & U_{ny} & U_{nz} \end{bmatrix}^T \end{aligned}. \quad (4)$$

The rotation vector in the body frame is expressed as:

$$\vec{\omega} = [\omega_x \quad \omega_y \quad \omega_z]^T, \quad \begin{cases} \omega_x = g_x - b_x \\ \omega_y = g_y - b_y \\ \omega_z = g_z - b_z \end{cases}, \quad (5)$$

where $\vec{g} = [g_x \quad g_y \quad g_z]$ is the gyroscope measurement, and $\vec{b} = [b_x \quad b_y \quad b_z]$ is the gyroscope bias. The state vector of the filter $\vec{X}$ consists of the attitude quaternion $\vec{q}$ and the gyroscope bias vector $\vec{b}$ as follows:

$$\vec{X} = [\vec{q} \quad \vec{b}]^T = [q_0 \quad q_1 \quad q_2 \quad q_3 \quad b_x \quad b_y \quad b_z]^T. \quad (6)$$

For the prediction of the next state, the derivative of $\vec{q}$ can be established as follows:

$$\dot{q} = \Omega[\vec{\omega}] \cdot \vec{q} = (0.5) \cdot \begin{bmatrix} 0 & -\vec{\omega}^T \\ \vec{\omega} & \vec{\omega}[\times] \end{bmatrix} \cdot \vec{q}, \quad (7)$$

where $\Omega[\vec{\omega}] = (0.5) \cdot \begin{bmatrix} 0 & -\omega_x & -\omega_y & -\omega_z \\ \omega_x & 0 & \omega_z & -\omega_y \\ \omega_y & -\omega_z & 0 & \omega_x \\ \omega_z & \omega_y & -\omega_x & 0 \end{bmatrix}$.

In (7), $\vec{\omega}[\times]$ denotes a 3×3 skew symmetric matrix. The discrete-time model corresponding to (7) is given as follows:

$$\vec{q}_{k+1} = \exp(\Omega_k \Delta t) \cdot \vec{q}_k, \quad (8)$$

where Δt is the system time interval. Therefore, the process model for EKF can be established as follows:

$$\begin{aligned} &\vec{X}_{k+1} = F \cdot \vec{X}_k \\ &\begin{bmatrix} \dot{q}_0 \\ \dot{q}_1 \\ \dot{q}_2 \\ \dot{q}_3 \\ \dot{b}_x \\ \dot{b}_y \\ \dot{b}_z \end{bmatrix} = \frac{\Delta t}{2} \begin{bmatrix} 1 & -\omega_x & -\omega_y & -\omega_z & q_1 & q_2 & q_3 \\ \omega_x & 1 & \omega_z & -\omega_y & -q_0 & q_3 & -q_2 \\ \omega_y & -\omega_z & 1 & \omega_x & -q_3 & -q_0 & q_1 \\ \omega_z & \omega_y & -\omega_x & 1 & q_2 & -q_1 & -q_0 \\ 0 & 0 & 0 & 0 & 1 & 0 & 0 \\ 0 & 0 & 0 & 0 & 0 & 1 & 0 \\ 0 & 0 & 0 & 0 & 0 & 0 & 1 \end{bmatrix} \begin{bmatrix} q_0 \\ q_1 \\ q_2 \\ q_3 \\ b_x \\ b_y \\ b_z \end{bmatrix} \end{aligned}, \quad (9)$$

where F is the Jacobian matrix, which propagates the covariance matrix.

The EKF process for the attitude estimation is illustrated in Fig. 1. For the pitch-roll estimation, the gravity vector can be used as an external reference for the correction of pitch and roll estimates [13] as shown in the figure. In Fig. 1, the quaternion for the pitch-roll estimation is denoted as $\vec{q}$. For the yaw estimation, the quaternion is updated using a low pass filter whose coefficient is calculated using the GPS sample time as follows:

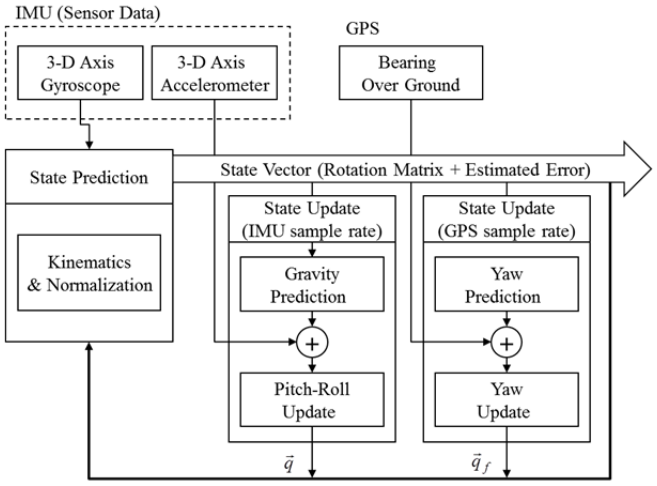

Fig. 1. The EKF process for the attitude estimation.

$$\vec{q}_f = \alpha \cdot \vec{q}_f + (1-\alpha)\cdot \vec{q} \qquad \alpha = e^{-\frac{\Delta t}{\tau+\Delta t}} \quad , \tag{10}$$

where τ is the GPS sample time, Δt is the IMU sample time, and $\vec{q}_f = [q_{f0} \quad q_{f1} \quad q_{f2} \quad q_{f3}]$ is the filtered quaternion vector.

The EKF process for the yaw estimation is given as follows:

Compute the estimated vector in the body frame:

$$Z_{Ye} = \begin{bmatrix} Z_{Ye1} \\ Z_{Ye2} \end{bmatrix} = \begin{bmatrix} 1-2(q_{f2}^2 + q_{f3}^2) \\ 2(q_{f1}q_{f2} + q_{f0}q_{f3}) \end{bmatrix}$$

Compute the yaw observation matrix:

$$H_Y = \frac{\partial}{\partial \vec{X}} Z_{Ye} = \begin{bmatrix} 0 & 0 & -4q_{f2} & -4q_{f3} & 0 & 0 & 0 \\ 2q_{f3} & 2q_{f2} & 2q_{f1} & 2q_{f0} & 0 & 0 & 0 \end{bmatrix}$$

Correct the magnitude of the GPS bearing over ground (χ) to calculate the measured vector in the body frame:

$$Z_{Ym} = \begin{bmatrix} \cos(\chi)\cdot\sqrt{{Z_{Ye1}}^2 + {Z_{Ye2}}^2} \\ \sin(\chi)\cdot\sqrt{{Z_{Ye1}}^2 + {Z_{Ye2}}^2} \end{bmatrix}$$

Compute the yaw error, covariance, and Kalman gain:

$$E_Y = Z_{Ym} - Z_{Ye},\ P_Y = H_Y \cdot P \cdot H_Y^T + R_Y,\ K_Y = P \cdot H_Y^T \cdot P_Y^{-1}$$

Update the system state:

$$X = X + K_Y \cdot E_Y$$

Update the system state covariance:

$$P = P - K_Y \cdot H_Y \cdot P$$

Using the filtered quaternion values, roll, pitch, and yaw can be computed as follows:

$$\begin{aligned} roll(\phi) &= \text{atan2}\left(2\left(q_{f2}q_{f3} + q_{f0}q_{f1}\right), 1-2\left(q_{f1}^2 + q_{f2}^2\right)\right) \\ pitch(\theta) &= \text{asin}\left(2\left(q_{f1}q_{f3} - q_{f0}q_{f2}\right)\right) \\ yaw(\psi) &= \text{atan2}\left(2\left(q_{f1}q_{f2} + q_{f0}q_{f3}\right), 1-2\left(q_{f2}^2 + q_{f3}^2\right)\right) \end{aligned} \quad . \tag{11}$$

This estimation work utilizes GPS information as well as inertial data for attitude estimation. Therefore, this work is not suitable for trajectory tracking in GPS-free environments.

B. Attitude Estimation Based On Quaternion

Section II-B describes another attitude estimation scheme [7], which is just based on quaternion. Therefore, this work is utilized for the proposed trajectory tracking estimator in GPS-free environments.

As stated in [7] and [14], the sensor models for gyroscope, accelerometer, and magnetometer are established, respectively as follows:

$$\begin{cases} \vec{\omega} = \mathrm{K}^g \vec{\omega}_{\text{true}} + \vec{\mathrm{b}}^g + \vec{\mathrm{v}}^g \\ \vec{\mathrm{a}} = \mathrm{K}^a [\mathrm{C}_n^b(\mathrm{q}) \cdot \vec{\mathrm{a}}_{\text{nav}}] + \vec{\mathrm{b}}^a + \vec{\mathrm{v}}^a \\ \vec{\mathrm{m}} = \mathrm{K}^m [\mathrm{C}_n^b(\mathrm{q}) \cdot \vec{\mathrm{h}}_{\text{nav}}] + \vec{\mathrm{b}}^m + \vec{\mathrm{v}}^m \end{cases} , \tag{12}$$

where K^g, K^a, and K^m are the scale factor matrices; $\vec{\mathrm{b}}^g$, $\vec{\mathrm{b}}^a$, and $\vec{\mathrm{b}}^m$ are the bias vectors; $\vec{\mathrm{v}}^g$, $\vec{\mathrm{v}}^a$, and $\vec{\mathrm{v}}^m$ are the measurement noises. In addition, $\vec{\omega}_{\text{true}}$ is the true rotational rate of IMU with respect to the inertial frame of reference in (12). From (7) and (12), $\Omega[\vec{\omega}]$ can also be defined as follows:

$$\Omega[\vec{\omega}] = 0.5 \cdot \begin{bmatrix} 0 & -(\omega_x + b_x^g) & -(\omega_y + b_y^g) & -(\omega_z + b_z^g) \\ (\omega_x + b_x^g) & 0 & (\omega_z + b_z^g) & -(\omega_y + b_y^g) \\ (\omega_y + b_y^g) & -(\omega_z + b_z^g) & 0 & (\omega_x + b_x^g) \\ (\omega_z + b_z^g) & (\omega_y + b_y^g) & -(\omega_x + b_x^g) & 0 \end{bmatrix} . \tag{13}$$

The relationship between quaternion and angular velocities is expressed as follows:

$$\begin{bmatrix} \dot{\mathrm{q}} \\ \dot{\mathrm{b}}^g \end{bmatrix} = 0.5 \cdot \begin{bmatrix} \Omega[\vec{\omega}] & \Xi \\ 0_{4\times3} & 0_{3\times3} \end{bmatrix} \cdot \begin{bmatrix} \vec{\mathrm{q}} \\ \vec{\mathrm{b}}^g \end{bmatrix} = 0.5 \cdot \begin{bmatrix} 0 & -\omega_x & -\omega_y & -\omega_z & -q_1 & -q_2 & -q_3 \\ \omega_x & 0 & \omega_z & -\omega_y & q_0 & -q_3 & q_2 \\ \omega_y & -\omega_z & 0 & \omega_x & q_3 & q_0 & -q_1 \\ \omega_z & \omega_y & \omega_x & 0 & -q_2 & q_1 & q_0 \\ 0 & 0 & 0 & 0 & 0 & 0 & 0 \\ 0 & 0 & 0 & 0 & 0 & 0 & 0 \\ 0 & 0 & 0 & 0 & 0 & 0 & 0 \end{bmatrix} \cdot \begin{bmatrix} q_0 \\ q_1 \\ q_2 \\ q_3 \\ b_x^g \\ b_y^g \\ b_z^g \end{bmatrix} . \tag{14}$$

The process model is established as follows:

$$\begin{aligned} \vec{\mathrm{X}}_k &= [\vec{\mathrm{q}}_k \quad \vec{\mathrm{b}}_k^a \quad \vec{\mathrm{b}}_k^m]^T \\ \vec{\mathrm{X}}_{k+1} &= \Phi(\Delta t, \vec{\omega}_k) \cdot \vec{\mathrm{X}}_k + \vec{\mathrm{w}}_k = \\ &\begin{bmatrix} \Phi(\Delta t, \vec{\omega}_k) + \mathrm{I}_{4\times4} & 0_{3\times4} & 0_{3\times4} \\ 0_{4\times3} & \mathrm{I}_{3\times3} & 0_{3\times3} \\ 0_{4\times3} & 0_{3\times3} & \mathrm{I}_{3\times3} \end{bmatrix} \cdot \begin{bmatrix} \vec{\mathrm{q}}_k \\ \vec{\mathrm{b}}_k^a \\ \vec{\mathrm{b}}_k^m \end{bmatrix} + \begin{bmatrix} \vec{\mathrm{w}}_k^q \\ \vec{\mathrm{w}}_k^a \\ \vec{\mathrm{w}}_k^m \end{bmatrix} \end{aligned} , \tag{15}$$

where $I_{n\times n}$ denotes $n\times n$ identity matrix, and the rest elements are defined as follows:

$$\Phi(\Delta t, \vec{\omega}_k) = (\Delta t/2)\cdot\Omega[\vec{\omega}_k]$$
$$\vec{w}_k^{\,q} = -(\Delta t/2)\cdot\Xi_k\cdot\sigma_w^g,\quad \vec{w}_k^{\,q} = \sigma_w^a,\quad \vec{w}_k^{\,m} = \sigma_w^m. \tag{16}$$

The *a priori* error covariance step of EKF is defined as follows: $P_{k+1}^- = \Phi(\Delta t, \vec{\omega}_k)\cdot P_k\cdot\Phi(\Delta t, \vec{\omega}_k)^T + Q_k$. The process noise covariance Q_k is expressed as follows:

$$Q_k = \begin{bmatrix} (\Delta t/2)^2\cdot\Xi_k\cdot{\sigma_w^g}^2\cdot\Xi_k^T & 0 & 0 \\ 0 & {\sigma_w^a}^2 & 0 \\ 0 & 0 & {\sigma_w^m}^2 \end{bmatrix}. \tag{17}$$

The measurement model can be constructed from the acceleration and the magnetic field strength as follows:

$$\vec{Z}_k = [\vec{a}_k \quad \vec{m}_k]^T,$$
$$\vec{Z}_k = F_k\vec{X}_k + \vec{v}_k = \begin{bmatrix} C_n^b(q_k) & 0 \\ 0 & C_n^b(q_k) \end{bmatrix}\cdot\begin{bmatrix}\vec{a}\\ \vec{h}\end{bmatrix} + \begin{bmatrix}\vec{v}_k^{\,a}\\ \vec{v}_k^{\,m}\end{bmatrix}. \tag{18}$$

The acceleration vector in the navigation frame is negligible compared to the gravity value ($g = 9.81$). Therefore, the measurement model associated with the acceleration can be expressed as follows:

$$Z^a(q) = C_n^b(q)\cdot\begin{bmatrix}0\\0\\-g\end{bmatrix} = \begin{bmatrix}-g(-2q_0q_2 + 2q_1q_3)\\ -g(2q_0q_1 + 2q_2q_3)\\ -g(2q_0^2 + 2q_3^2 - 1)\end{bmatrix}. \tag{19}$$

The equation (19) can be converted into Jacobian form by taking a partial derivative with regards to the quaternion:

$$J^a(q) = \frac{\partial Z^a(q)}{\partial(q)} = \begin{bmatrix} 2gq_2 & -2gq_3 & 2gq_0 & -2gq_1 \\ -2gq_1 & -2gq_0 & -2gq_3 & -2gq_2 \\ -4gq_0 & 0 & 0 & -4gq_3 \end{bmatrix}. \tag{20}$$

For the magnetometer measurement model, the normalized magnetic field measurement vector ($\vec{m}$) is rotated into $\vec{b}$ as follows [9]:

$$\vec{m} = [m_x \quad m_y \quad m_z],$$
$$\vec{b} = [0 \quad b_x \quad b_y \quad b_z] = \vec{q}\otimes\vec{m}\otimes\vec{q}^{-1}, \tag{21}$$

where $\vec{m}$ is calibrated using the scheme in [15]. In (18), the earth's magnetic field ($\vec{h}$) is defined as follows:

$$\vec{h} = [h_x \quad h_y \quad h_z] = [\sqrt{b_x^2 + b_y^2} \quad 0 \quad b_z]. \tag{22}$$

The measurement model for magnetic field can be expressed as follows:

$$Z^m(q) = C_n^b(q)\cdot\vec{h} =$$
$$\begin{bmatrix} h_x(2q_0^2 + 2q_1^2 - 1) + h_y(2q_0q_3 + 2q_1q_2) + h_z(-2q_0q_2 + 2q_1q_3) \\ h_x(-2q_0q_3 + 2q_1q_2) + h_y(2q_0^2 + 2q_2^2 - 1) + h_z(2q_0q_1 + 2q_2q_3) \\ h_x(2q_0q_2 + 2q_1q_3) + h_y(-2q_0q_1 + 2q_2q_3) + h_z(2q_0^2 + 2q_3^2 - 1)\end{bmatrix}. \tag{23}$$

The Jacobian form for magnetic field is expressed as:

$$J^m(q) = \frac{\partial Z^m(q)}{\partial(q)} =$$
$$\begin{bmatrix} 4h_xq_0 - 2h_zq_2 + 2h_yq_3 & 4h_xq_1 - 2h_yq_2 + 2h_zq_3 \\ 4h_yq_0 + 2h_zq_1 - 2h_xq_3 & 2h_zq_0 + 2h_xq_2 \\ 4h_zq_0 - 2h_yq_1 + 2h_xq_2 & -2h_yq_0 + 2h_xq_3 \end{bmatrix}. \tag{24}$$
$$\begin{bmatrix} -2h_zq_0 + 2h_yq_1 & 2h_yq_0 + 2h_zq_1 \\ 2h_xq_1 + 4h_yq_2 + 2h_zq_3 & -2h_xq_0 + 2h_zq_2 \\ 2h_xq_0 + 2h_yq_3 & 2h_xq_1 + 2h_yq_2 + 4h_zq_3 \end{bmatrix}$$

Using (19), (20), (23), and (24), the measurement model Z_k (which consists of acceleration and magnetic field strength) and the Jacobian matrix F_k can be established as follows:

$$Z_k = \begin{bmatrix} Z^a(q_k)\\ Z^m(q_k)\end{bmatrix},\quad F_k = \begin{bmatrix} J^a(q_k) & I_{3\times3} & 0_{3\times3} \\ J^m(q_k) & 0_{3\times3} & I_{3\times3}\end{bmatrix}. \tag{25}$$

The measurement noises of the accelerometer and the magnetometer $\vec{v}_k^{\,a}$ and $\vec{v}_k^{\,m}$ are uncorrelated white noise processes with the following covariance matrix:

$$R_k = \begin{bmatrix} R_k^a & 0 \\ 0 & R_k^m\end{bmatrix} = \begin{bmatrix} {\sigma_v^a}^2\cdot I_{3\times3} & 0_{3\times3} \\ 0_{3\times3} & {\sigma_v^m}^2\cdot I_{3\times3}\end{bmatrix}. \tag{26}$$

Table I exhibits the parameter values for the simulation of the attitude estimation based on quaternion. The standard deviation values for the process and the measurement noises are given in Table I.

TABLE I
THE PARAMETER VALUES FOR THE SIMULATION OF THE ATTITUDE ESTIMATION BASED ON QUATERNION

Process Noise			Measurement Noise	
σ_w^g	σ_w^a	σ_w^m	σ_v^a	σ_v^m
[rad/s]	[m/s^2]	[tesla]	[m/s^2]	[tesla]
0.8	0.5	0.05	0.2	0.1

Fig. 2 shows the estimated attitude values [roll (ϕ), pitch (θ), and yaw (ψ)] in the simulation. The EKF determines the quaternion information using angular velocities, accelerations and magnetic readings from a sensor device. Then, the attitude values are estimated using the quaternion information as indicated in (11). For the simulation, the sensor device is rotated by $\pi/2$, and then rotated by $-\pi$ in the x axis. Finally, the sensor device is rotated into the starting position. The sensor device also performs the same rotations in y and z axes [9]. Fig. 2 indicates that the estimated attitude values accurately follow the rotations of the sensor device. Fig. 2 confirms that this related work can produce the vehicle attitude without GPS. However, even with this attitude estimator, the conventional navigation systems still rely on GPS in order to achieve the vehicle speed, which is required for the estimation of vehicle positions.

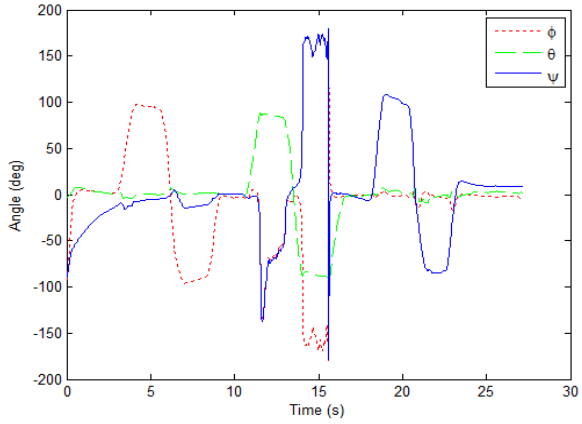

Fig. 2. The estimated attitude values (roll/pitch/yaw) in the simulation.

III. Proposed Estimator For Trajectory Tracking

Fig. 3 illustrates the architecture of the proposed estimator for trajectory tracking in GPS-free environments. As shown in the figure, the presented estimator consists of extended Kalman filter (EKF) and linear Kalman filter. The EKF receives the inertial sensor data from the low-cost IMU, which consists of gyroscope, magnetometer, and accelerometer as shown in Fig. 3. The inertial sensor data includes angular velocity, magnetic field strength, and acceleration information, which are produced by the gyroscope, the magnetometer, and the accelerometer, respectively in the IMU.

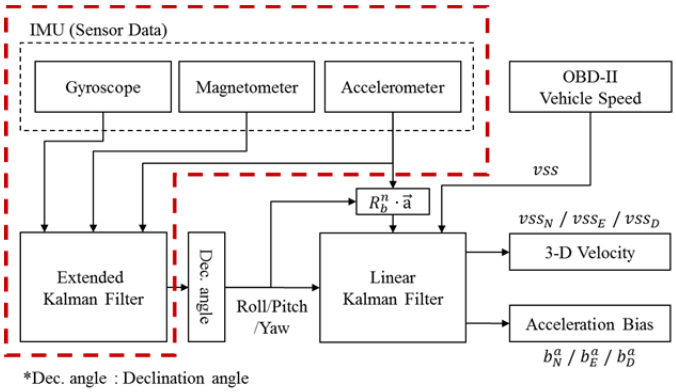

Fig. 3. The architecture of the proposed estimator for trajectory tracking.

Using the inertial sensor data, the EKF estimates the vehicle attitude (roll/pitch/yaw) as stated in section II-B (the bold dash line in Fig. 3). Using the estimated roll/pitch/yaw angles, the rotation matrix of (2) can be transformed into the trigonometric function matrix as follows [16]:

$$R_n^b = \begin{bmatrix} R_{11} & R_{12} & R_{13} \\ R_{21} & R_{22} & R_{23} \\ R_{31} & R_{32} & R_{33} \end{bmatrix} = \begin{bmatrix} c_\theta c_\psi & c_\theta s_\psi & -s_\theta \\ s_\varphi s_\theta c_\psi - c_\varphi s_\psi & s_\varphi s_\theta s_\psi + c_\varphi c_\psi & c_\theta s_\varphi \\ c_\varphi s_\theta c_\psi + s_\varphi s_\psi & c_\varphi s_\theta s_\psi - s_\varphi c_\psi & c_\theta c_\varphi \end{bmatrix}, \quad (27)$$

where s_* and c_* denote sin(*) and cos(*), and $[\phi \quad \theta \quad \psi]$ are roll, pitch, and yaw angles, respectively. In Fig. 3, the OBD-II produces the vehicle speed (vss) in the body frame. Using the vehicle speed in the body frame, the velocity and the acceleration in the NED frame can be calculated as follows [17]:

$$vss_{NED} = R_b^n \cdot vss_{BODY}, \quad \vec{a}_{NED} = R_b^n \cdot \vec{a}, \quad (28)$$

where $vss_{NED} = [v_N \quad v_E \quad v_D]^T$, $vss_{BODY} = [v_x \quad v_y \quad v_z]^T$, $\vec{a}_{NED} = [a_N \quad a_E \quad a_D]^T$ and $R_b^n = (R_n^b)^T$. When the vehicle moves in a straight line, only the direction of the X-body vector is measured. In other words, the measurement values are zeros in the Y-body and the Z-body vectors. Therefore, the north velocity (v_N), the east velocity (v_E), and the down velocity (v_D) can simply be calculated in the NED frame as follows:

$$\begin{aligned} v_N &= vss \times \left(R_{11} \Big/ \sqrt{(R_{11})^2 + (R_{12})^2 + (R_{13})^2} \right) \\ v_E &= vss \times \left(R_{12} \Big/ \sqrt{(R_{11})^2 + (R_{12})^2 + (R_{13})^2} \right) \\ v_D &= vss \times \left(R_{13} \Big/ \sqrt{(R_{11})^2 + (R_{12})^2 + (R_{13})^2} \right) \end{aligned}. \quad (29)$$

Note that the speed values of (29) include some bias terms due to gravity contribution. Therefore, the linear Kalman filter (LKF) is required in order to eliminate the bias terms as shown in Fig. 3.

A. Process Model for LKF

The mathematical relation between velocity and acceleration in the NED frame is modeled as follows:

$$vss_{k+1} = vss_k + (a_k - b_k^a) \cdot \Delta t + v_k, \quad (30)$$

where vss_k, a_k, Δt, and v_k are the current vehicle speed, acceleration, time interval, and measurement noise, respectively, and b_k^a denotes the acceleration bias due to gravity contribution. Based on the expression of (30), the process model for the LKF can be established in detail as follows:

$$\begin{bmatrix} v_N \\ v_E \\ v_D \\ b_N^a \\ b_E^a \\ b_D^a \end{bmatrix}_{k+1} = \begin{bmatrix} 1 & 0 & 0 & -\Delta t & 0 & 0 \\ 0 & 1 & 0 & 0 & -\Delta t & 0 \\ 0 & 0 & 1 & 0 & 0 & -\Delta t \\ 0 & 0 & 0 & 1 & 0 & 0 \\ 0 & 0 & 0 & 0 & 1 & 0 \\ 0 & 0 & 0 & 0 & 0 & 1 \end{bmatrix} \begin{bmatrix} v_N \\ v_E \\ v_D \\ b_N^a \\ b_E^a \\ b_D^a \end{bmatrix}_k + \begin{bmatrix} \Delta t \\ \Delta t \\ \Delta t \\ 0_{3\times 1} \end{bmatrix} \begin{bmatrix} a_N & a_E & a_D & 0_{1\times 3} \end{bmatrix}_k + \begin{bmatrix} \sigma_w^{vss\,2} \cdot \mathrm{I}_{3\times 3} & 0_{3\times 3} \\ 0_{3\times 3} & \sigma_w^{b\,2} \cdot \mathrm{I}_{3\times 3} \end{bmatrix} \quad . (31)$$

The expression of (31) can be compacted into a vector form as follows:

$$\vec{x}_{k+1} = A_k \vec{x}_k + B_k u_k + W_k, \quad (32)$$

where A_k, B_k, and W_k denote the state transition model, the control input model, and the process noise model, respectively.

B. Measurement Model for LKF

The measurement model for the LKF of Fig. 3 can be established as follows:

$$z_k = H_k x_k + v_k$$

$$z_k = \begin{bmatrix} I_{3\times3} & 0_{3\times3} \\ 0_{3\times3} & 0_{3\times3} \end{bmatrix} \begin{bmatrix} v_N \\ v_E \\ v_D \\ b_N^a \\ b_E^a \\ b_D^a \end{bmatrix}_k + \begin{bmatrix} \sigma_v^{vss\,2} \cdot I_{3\times3} & 0_{3\times3} \\ 0_{3\times3} & \sigma_v^{b\,2} \cdot I_{3\times3} \end{bmatrix}. \quad (33)$$

The prediction and the update phases for the LKF are summarized in [18].

Table II includes the standard deviations of the process and the measurement noises for the LKF. Fig. 4 exhibits the simulation results of the random vehicle movement for the proposed estimator in real environments. The results include the estimated north, the estimated east, and the estimated down velocities.

TABLE II
THE PARAMETER VALUES OF THE LKF

Process Noise		Measurement Noise	
σ_w^{vss} [m/s]	σ_w^b [m/s^2]	σ_v^{vss} [m/s]	σ_v^b [m/s^2]
0.06	0.006	0.2	0.02

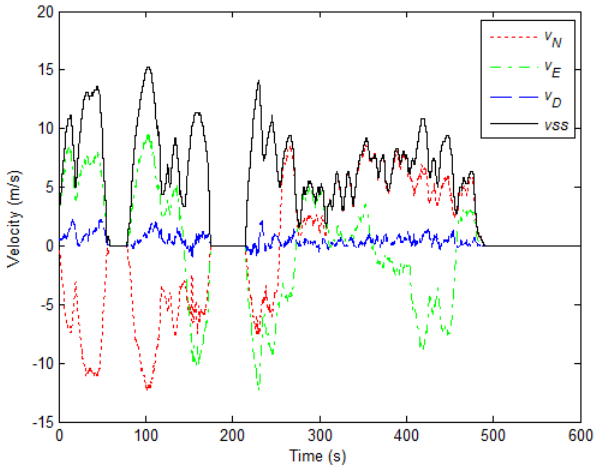

Fig. 4. The estimated north velocity (v_N), east velocity (v_E), down velocity (v_D), and the measured vehicle speed (vss)

IV. EXPERIMENTAL EVALUATION

Experimental evaluation exhibits the effectiveness of the proposed tracking estimator. For the verification of the proposed estimator system, the position estimates of the presented system are compared with those of GPS in this section.

The GPS generates the filtered velocity vector in earth-centered and earth-fixed (ECEF) frame, and the longitude/latitude information. Fig. 5 illustrates the architecture of the verification model for the proposed estimator system. In the figure, the GPS resolves the velocity vector in the ECEF XYZ reference frame and the direction (longitude/latitude). Then, the ECEF velocity vector is transformed into the velocity vector (north/east/down velocities) in the NED frame. The NED velocity vector is consistent with the geodetic longitude/latitude/altitude (LLA) information. For the transformation of the ECEF velocity vector into the NED velocity vector, the following rotation matrix is utilized:

$$v_{NED} = R_{ecef}^{ned} \cdot v_{ECEF}$$

$$\begin{bmatrix} v_{north} \\ v_{east} \\ v_{down} \end{bmatrix} = \begin{bmatrix} -\sin\varphi\cos\lambda & -\sin\varphi\sin\lambda & \cos\varphi \\ -\sin\lambda & \cos\lambda & 0 \\ -\cos\varphi\cos\lambda & -\cos\varphi\sin\lambda & -\sin\varphi \end{bmatrix} \begin{bmatrix} v_X \\ v_Y \\ v_Z \end{bmatrix}, \quad (34)$$

where v_X, v_Y and v_Z are the velocities in the ECEF frame, and φ and λ are geodetic latitude and longitude, respectively.

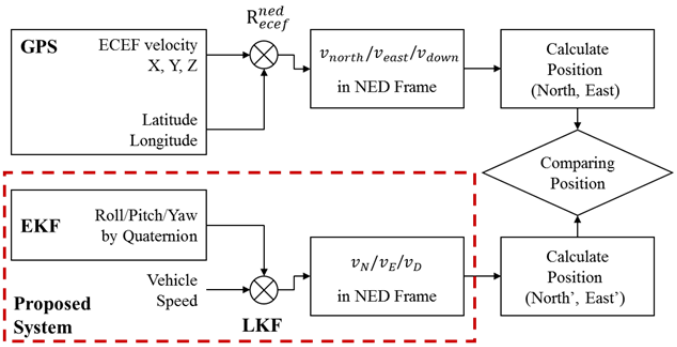

Fig. 5. The architecture of the verification model for the proposed system.

Fig. 6 illustrates the test facility for the verification model of Fig. 5. The test facility is set up inside a vehicle as depicted in Fig. 6. The test facility consists of a GPS receiver, a low-cost IMU orientation sensor, and an embedded board. The GPS receiver is utilized for the comparison of the proposed estimator as indicated in Fig. 5. The IMU sensor delivers the inertial sensor data (such as angular velocity, magnetic field strength,

Fig. 6. The test facility for the verification model of the proposed estimator.

and acceleration information) to the embedded board. In order to obtain the vehicle speed from the OBD-II, the embedded board is also interfaced to the OBD-II data link connector using the controller area network (CAN) protocol. Using the IMU sensor and the OBD-II, the embedded board acquires the measurements for the vehicle attitude (roll/pitch/yaw in Fig. 5) and the velocity speed, respectively. Two road tests (track #1 and track #2) were performed by driving the vehicle equipped with the test facility of Fig. 6. The test driving distances of track #1 and track #2 are 3.47 km and 3.93 km, respectively. Fig. 7 shows the real road environment of track #1.

Fig. 7. The real road environment of track #1 for the verification of the proposed estimator: the ground truth (solid line) of the vehicle trajectory.

Fig. 8 shows a comparison of the ground truth, the position estimates of the GPS, and the position estimates of the proposed estimator in the real road environment of Fig. 7. In Fig. 8, the position estimates are calculated using the estimated NED velocity vector as follows:

$$\mathrm{POS}_{\mathrm{EAST/NORTH}}(t) = \sum_{t=0}^{n-1} \Delta t \cdot v_{EAST/NORTH}(t), \qquad (35)$$

where $v_{EAST}(t) = v_{east}(t), v_{NORTH}(t) = v_{north}(t)$ in the case of GPS, and $v_{EAST}(t) = v_E(t), v_{NORTH}(t) = v_N(t)$ in the case of the proposed system. As indicated in Fig. 8, the position estimates of the proposed estimator are closer to the positions of the ground truth.

Table III exhibits a comparison of the root mean-squared error (RMSE) performance for the proposed estimator and the GPS receiver. In the table, the RMSE is calculated as follows:

$$\mathrm{RMSE}_{\mathrm{E/N}} = \mathrm{sqrt}\left(\sum_{t=0}^{n-1} \left(\mathrm{POS}^{\mathrm{GT}}_{\mathrm{E/N}}(t) - \mathrm{POS}_{\mathrm{E/N}}(t) \right)^2 / n \right), \qquad (36)$$

$$\mathrm{RMSE} = \mathrm{sqrt}\left(\left(\mathrm{RMSE}_{\mathrm{E}}^2 + \mathrm{RMSE}_{\mathrm{N}}^2 \right) / 2 \right)$$

where $\mathrm{POS}^{\mathrm{GT}}_{\mathrm{E/N}}$ denotes the east or the north position of the ground truth. As shown in Table III, the proposed estimator is superior to the GPS receiver in the RMSE performance. As indicated in the table, GPS receivers usually give poor accuracy in the position estimation since GPS signals frequently suffer from signal fading.

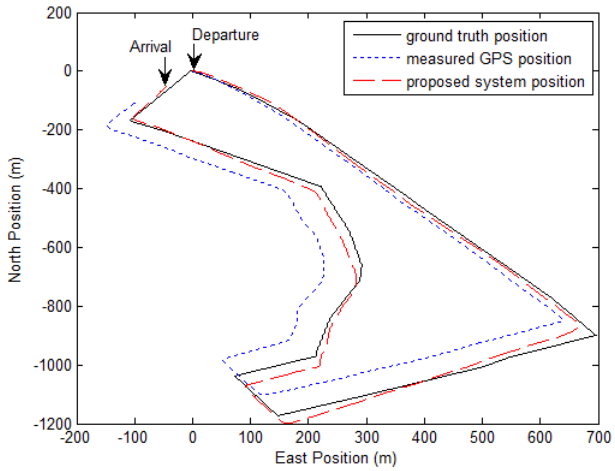

Fig. 8. The comparison of the ground truth, the position estimates of the GPS, and the position estimates of the proposed estimator.

TABLE III
THE COMPARISON OF THE RMSE PERFORMANCE FOR THE PROPOSED ESTIMATOR AND THE GPS RECEIVER

Track No.	GPS Measurement (m)	Proposed Estimator (m)
Track #1	56.3465	28.8604
Track #2	37.0584	34.7338

For further evaluation of the proposed estimator, the presented estimator is compared with the conventional estimator (section II-A). The convention estimator integrates vehicle attitude and GPS information. The conventional version achieves the vehicle attitude and the filtered vehicle speed using the quaternion-based method (section II-A) and the GPS receiver, respectively.

Fig. 9 exhibits a comparison of the ground truth, the position estimates of the related-work (section II-A) based conventional estimator, and the position estimates of the proposed estimator in the real road environment of Fig. 7. In the related-work based system, the GPS signal is available during the entire travel time of the vehicle. Fig. 9 reveals that the position estimates of the proposed estimator are also closer to the positions of the ground truth than those of the related-work based conventional estimator. This is due to the fact that the GPS fading may reduce the position accuracy even in the conventional estimator.

Fig. 10 exhibits a comparison of the ground truth, and the position estimates of the related-work (section II-A) based conventional estimator in the GPS-available case and in the GPS-outage case in the real road environment of Fig. 7. The GPS-available case indicates that the GPS signal is available during the entire travel time of the vehicle. On the other hand, the GPS-outage case indicates that the GPS signal is unavailable during about 2.2% of the entire travel time. As

shown in Fig. 10, the position estimates of the GPS-available case are a little closer to the positions of the ground truth than those of the GPS-outage case. In other words, the GPS performance affects the performance of the conventional estimator.

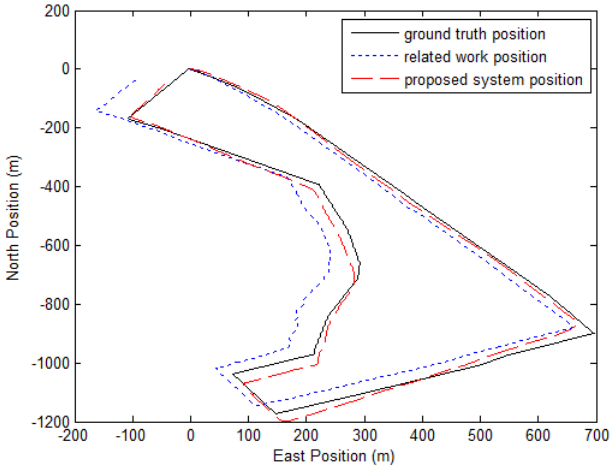

Fig. 9. The comparison of the ground truth, the position estimates of the related-work (section II-A) based conventional estimator, and the position estimates of the proposed estimator.

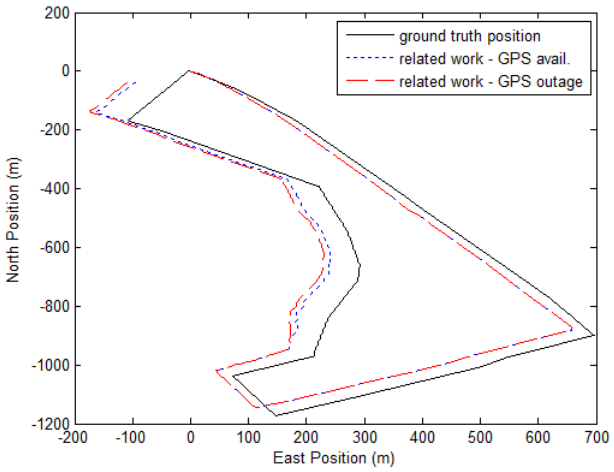

Fig. 10. The comparison of the ground truth, and the position estimates of the related-work (section II-A) based conventional estimator in the GPS-available case and in the GPS-outage case.

Table IV exhibits a comparison of the RMSE performance for the proposed estimator and the related-work (section II-A) based conventional estimator. As shown in the table, the proposed estimator outperforms the conventional estimator even in the case that the GPS signal is available during the entire travel time. The GPS usually suffers from signal fading, which may lessen the accuracy of the vehicle speed. Note that the conventional estimator utilizes the filtered vehicle speed from the GPS receiver. On the other hand, the proposed estimator achieves the vehicle speed from the OBD-II, and then refines the NED velocity vector further using the vehicle speed and the LKF, which leads to better RMSE performance in Table IV. The track #1 of this table also confirms the experiment results of Figs. 9 and 10. In the comparison of Tables III and IV, the conventional estimator is superior to the GPS receiver in the RMSE performance. Since the conventional version fuses the IMU sensor data and the GPS information, its RMSE performance is better than that of the GPS. Table IV also reveals that the GPS outage worsens the performance of the related-work based conventional estimator.

TABLE IV
THE COMPARISON OF THE RMSE PERFORMANCE FOR THE PROPOSED ESTIMATOR AND THE RELATED-WORK (SECTION II-A) BASED CONVENTIONAL ESTIMATOR

Track No.	Proposed Estimator (m)	The Related Work (m)	
		GPS Available	GPS Outage
Track #1	28.8604	43.6983	47.7642
Track #2	34.7338	36.1626	36.6098

V. CONCLUSION

This paper proposes a consumer tracking estimator for vehicles in GPS-free environments. Unlike the conventional estimators, the novel estimator never relies on the GPS. The proposed estimator exploits the low-cost IMU sensor and the OBD-II in order to achieve navigation information without any aid of GPS. The estimator achieves the inertial data (angular velocity, magnetic field strength, and acceleration information) and the vehicle speed from the IMU and the OBD-II, respectively. Then, the estimator relies on the EKF algorithm, which produces the vehicle attitude (roll/pitch/yaw) using the inertial data. The novel estimator also utilizes the LKF algorithm, which accurately estimates the NED velocity vector using the vehicle attitude and the vehicle speed. The presented estimator finally calculates the vehicle position using the estimated NED velocity vector.

Experimental evaluation shows that the proposed tracking estimator is superior to the GPS receiver and the conventional estimator (which is partially based on the GPS) in the tracks (track #1 and track #2). The RMSE results also confirm that the presented estimator outperforms the GPS receiver and the conventional estimator. This reveals that the proposed tracking estimator is more suitable for consumer navigation system and advanced driver assistance system (ADAS).

REFERENCES

[1] I. Jeon, M. Song, S. Chang, S. J. Choi, and Y.-T. Lee, "A signaling emergency alert system multiplexed with T-DMB channel for emergency alert service," *IEEE Trans. Consumer Electron.*, vol. 61, no. 1, pp. 16-23, Feb. 2015.

[2] S.-Y. Jung, S. Hann, and C.-S. Park, "TDoA-based optical wireless indoor localization using LED ceiling lamps," *IEEE Trans. Consumer Electron.*, vol. 57, no. 4, pp. 1592–1597, Nov. 2011.

[3] H. Cho, H. Jang, and Y. Baek, "Practical localization system for consumer devices using zigbee networks," *IEEE Trans. Consumer Electron.*, vol. 56, no. 3, pp. 1562–1569, Aug. 2010.

[4] E. H. Shin, "Estimation techniques for low-cost inertial navigation," Ph.D. dissertation, Dept. Geo. Eng., Univ. Calgary, Calgary, AB, 2005.

[5] Y. Girardin, M. Walsh, J. Torres, J. Barton, B, O'Flynn, and C. O'Mathuna, "Accounting for sensor drift in miniature, Wireless inertial measurement and positioning system: An extended Kalman filtering approach," in *Proc. IET ISSC 2010,* Cork, 2010, pp. 255–260.

[6] G. Sato, T. Asai, T. Sakamoto, and T. Hase, "Improvement of the positioning accuracy of a software-based GPS receiver using a 32-bit embedded microprocessor," *IEEE Trans. Consumer Electron.,* vol. 46, no. 3, pp. 521–530, Aug. 2000.

[7] A. M. Sabatini, "Quaternion-based extended Kalman filter for determining orientation by inertial and magnetic sensing," *IEEE Trans. Biomed. Eng.,* vol. 53, no. 7, pp. 1346–1356, Jun. 2006.
[8] B. Lee, W. C. Bang, James D. K. Kim, and C. Y. Kim, "Orientation estimation in mobile virtual environments with inertial sensors," *IEEE Trans. Consumer Electron.,* vol. 57, no. 2, pp. 802–810, Jul. 2011.
[9] S. O .H. Madgwick, A. J. L. Harrison, and R. Vaidyanathan, "Estimation of IMU and MARG orientation using a gradient descent algorithm," in *Proc.2011 IEEE Int. Conf. ICORR,* Zurich, 2011, pp. 1–7.
[10] *OBD II Scan Tool Equivalent to ISO/DIS 15031-4,* SAE Standard J1978 199203, 2001.
[11] R. Malekian, N. R. Moloisane, L. Nair, B.T. Maharaj, and U. A. K. Chude-Okonkwo, "Design and implementation of a wireless OBD II fleet management system," *IEEE Sensors J.,* vol. 17, no. 4, pp. 1154-1164, Feb. 2017.
[12] J. E. Meseguer, C. T. Calafate, J. C. Cano, and P. Manzoni, "Assessing the impact of driving behavior on instantaneous fuel consumption," in *Proc. 12th Annu. IEEE Consumer Comm. and Net. Conf. (CCNC)*, Las Vegas, 2015, pp. 443-448.
[13] R. Munguia and A. Grau, "Closing loops with a virtual sensor based on monocular SLAM," *IEEE Trans. Instrum. and Meas*, vol. 58, no. 8, pp. 2377-2384, Aug. 2009.
[14] I. Skog and P. Handel, "Calibration of a MEMS inertial measurement unit," in *Proc. XVII IMEKO World Congr.,* Rio de Janeiro, 2006, pp. 17–22.
[15] J. M. G. Merayo, P. Brauer, F. PrimdalI, J. R. Retersen, and O. V. Nielsen, "Scalar calibration of vector magnetometers," *Meas. Sci. and Technol.,* vol. 11, no. 2, pp. 120-132, Feb. 2000.
[16] J. Diebel, "Representing attitude: Euler angles, unit quaternions, and rotation vectors," *Matrix,* vol. 58, pp. 11, 2006.
[17] G. Cai, B. M. Chen, and T. H. Lee, "Coordinate systems and transformations," in *Unmanned rotorcraft systems,* 1st ed., New York: Springer Science & Business Media, 2011, ch. 2, pp. 33-34.
[18] R. E. Kalman, "A new approach to linear filtering and prediction problems," *J. of Basic Eng.*, vol. 82, no. 1, pp. 34-45, Mar. 1960.

Eunseok Choi received the B.S.E.E & M.S.E.E. degrees from the Department of Electronics and Information Engineering, Korea Aerospace University, Goyang, Korea, in 2000 and 2002, respectively. He is currently pursuit of Ph.D. degree at the Department of Electrical and Computer Engineering, the University of Seoul, Seoul, Korea. He is also working for SK Holdings, Seongnam, Korea. His current research interests include real-time locating systems, internet-of-things, embedded vehicle systems, and renewable energy systems.

Sekchin Chang received the B.S.E.E and M.S.E.E. degrees from the Department of Electronics and Computer Engineering, Korea University, Seoul, Korea, in 1991 and 1993, respectively, and the Ph.D. degree from the Department of Electrical and Computer Engineering, the University of Texas at Austin, TX, USA, in 2001. From 1993 to 1998, he was with Electronics and Telecommunications Research Institute (ETRI), Daejon, Korea. He was also with Motorola, Inc., Austin, TX, USA, from 2000 to 2004. Since February 2004, he has been with the Department of Electrical and Computer Engineering, the University of Seoul, Seoul, Korea, where he is currently a full professor. His current research interests include real-time locating systems, internet-of-things, embedded vehicle systems, and wireless communications.